The five homologous CiaR-controlled Ccn sRNAs of *Streptococcus pneumoniae* modulate Zn-resistance.

Nicholas R. De Lay[1,4#], Nidhi Verma[1], Dhriti Sinha[1], Abigail Garrett[2], Maximillian K. Osterberg[3], Spencer Reiling[1], Daisy Porter[1], David P. Giedroc[3], and Malcolm E. Winkler[2]

[1]Department of Microbiology and Molecular Genetics, McGovern Medical School, University of Texas Health Science Center, Houston, TX 77030, USA

[2]Department of Biology, Indiana University Bloomington, Bloomington, Indiana 47405

[3]Department of Chemistry, Indiana University, Bloomington, Bloomington, Indiana 47405

[4]MD Anderson Cancer Center UTHealth Graduate School of Biomedical Sciences, University of Texas Health Science Center, Houston, TX 77030, USA

Running Title: Loss of the Ccn sRNAs cause Zn hypersensitivity

Keywords: small RNA; post-transcriptional regulation; Zn homeostasis; Mn homeostasis; CiaRH

[#] Correspondence should be sent to Nicholas R. De Lay (Tel: +1 (713) 500-6293; Email: nicholas.r.delay@uth.tmc.edu)

ABSTRACT

Zinc is a vital transition metal for *Streptococcus pneumoniae*, but is deadly at high concentrations. In *S. pneumoniae*, elevated intracellular free Zn levels result in mis-metallation of key Mn-dependent metabolic and superoxide detoxifying enzymes resulting in Zn intoxication. Here, we report our identification and characterization of the function of the five homologous, CiaRH-regulated Ccn sRNAs in controlling *S. pneumoniae* virulence and metal homeostasis. We show that deletion of all five *ccn* genes (*ccnA*, *ccnB*, *ccnC*, *ccnD*, and *ccnE*) from *S. pneumoniae* strains D39 (serotype 2) and TIGR4 (serotype 4) causes Zn hypersensitivity and an attenuation of virulence in a murine invasive pneumonia model. We provide evidence that bioavailable Zn disproportionately increases in *S. pneumoniae* strains lacking the five *ccn* genes. Consistent with a response to Zn intoxication or relatively high intracellular free Zn levels, expression of genes encoding the CzcD Zn exporter and the Mn-independent ribonucleotide reductase, NrdD-NrdG, were increased in the Δ*ccnABCDE* mutant relative to its isogenic *ccn*$^+$ parent strain. The growth inhibition by Zn that occurs as the result of loss of the *ccn* genes is rescued by supplementation with Mn or Oxyrase™, a reagent that removes dissolved oxygen. Lastly, we found that the Zn-dependent growth inhibition of the Δ*ccnABCDE* strain was not altered by deletion of *sodA*, whereas the *ccn*$^+$ Δ*sodA* strain phenocopied the Δ*ccnABCDE* strain. Overall, our results indicate that the Ccn sRNAs have a crucial role in preventing Zn intoxication in *S. pneumoniae*.

AUTHOR SUMMARY

Zn and Mn are essential micronutrients for many bacteria, including *Streptococcus pneumoniae*. While Zn performs vital structural or catalytic roles in certain proteins, in excess, Zn can inhibit Mn uptake by *S. pneumoniae* and displace, but not functionally replace Mn from key enzymes including superoxide dismutase A (SodA). Here, we show that the Ccn small regulatory RNAs

promote *S. pneumoniae* resistance to Zn intoxication. Furthermore, we demonstrate that these small regulatory RNAs modulate the ability of *S. pneumoniae* to cause invasive pneumonia. Altogether, these findings reveal a new layer of regulation of *S. pneumoniae* Zn homeostasis and suggest that there are factors in addition to known transporters that modulate intracellular, bioavailable Zn levels.

INTRODUCTION

Small regulatory RNAs have been established as fundamental regulators of gene expression in bacteria and are involved in controlling nearly every aspect of bacterial physiology, metabolism, and behavior (*1-3*). Two basic classes of small regulatory RNAs have been identified and characterized, those that control gene expression by directly interacting with transcripts via hydrogen bonding between complementary or wobble base-pairs and others that indirectly effect transcript abundance by titrating an RNA or DNA-binding protein (*4, 5*). Interactions between the former class of riboregulators, henceforth referred to as sRNAs, and their cognate target transcripts can result in changes in mRNA transcription, translation, and/or stability depending on many factors including the sequence, accessibility, structure, and location of the sRNA binding site. One of the most facile modes of regulation discovered involves the sRNA binding within or adjacent to the translation initiation region blocking the 16S rRNA within the 30S ribosomal subunit from base-pairing with the complementary Shine-Delgarno sequence, or ribosome binding site, within the mRNA. Many other elegant mechanisms of sRNA-based gene regulation have been uncovered (*6-8*). While a large amount of progress has been made towards understanding the contribution of sRNAs to the response of Gram-negative bacteria such as *Escherichia coli* to internally and externally derived stresses, environmental cues, and host interactions, much less headway has been achieved in understanding the functions of sRNAs in Gram-positive bacteria, particularly, *Streptococcus pneumoniae* (pneumococcus).

77 The Gram-positive, ovoid diplococcus *S. pneumoniae* is a leading cause of lower respiratory
78 infection morbidity and mortality worldwide resulting in nearly 2 million deaths per year (*9*). We
79 and others have discovered 100s of putative sRNAs in *S. pneumoniae* (*10-15*), but the functions
80 of almost all of them remains a mystery. Among the first sRNAs identified in *S. pneumoniae*
81 were the five homologous Ccn sRNAs (CcnA, CcnB, CcnC, CcnD, and CcnE), which were
82 shown to be transcribed in response to activation of the CiaRH two-component system (*15, 16*);
83 expression of the CiaRH two-component systems is induced by penicillin and sialic acid (*17,*
84 *18*). Shortly after the discovery of the five Ccn sRNAs, Tsui, Mukerjee (Sinha), et al
85 demonstrated that CcnA negatively regulates competence and the *comCDE* mRNA encoding
86 the precursor of the competence stimulating peptide and the two-component system that
87 responds to this signal and activates competence (*15*). Schnorpfeil et al formally demonstrated
88 that the five Ccn sRNAs negatively regulate competence by base-pairing with the *comCDE*
89 mRNA (*19*). Other likely targets post-transcriptionally regulated by the Ccn sRNAs were
90 identified in that study including mRNAs encoding components of a galactose transporter
91 (*spd_0090*), a formate-nitrate transporter (*nirC*), branched-chain amino acid transporter (*brnQ*)
92 and a toxin *(shetA*), but direct regulation of these targets by the Ccn sRNAs has not yet been
93 established (*19*). One of these five homologous sRNAs, CcnE, has also been implicated in *S.*
94 *pneumoniae* strain TIGR4 virulence in a murine invasive pneumonia model (*12*).
95 Here, we report our discovery of a role for the five Ccn sRNAs in controlling *S. pneumoniae*
96 virulence and Zn resistance. Specifically, we show that deletion of the genes encoding the five
97 Ccn sRNAs attenuates the virulence of *S. pneumoniae* strains D39 and TIGR4 in a murine
98 invasive pneumonia model. Additionally, we show that loss of the Ccn sRNAs leads *S.*
99 *pneumoniae* D39 and TIGR4 to become hypersensitive to Zn toxicity, and this Zn
100 hypersensitivity is alleviated by supplementation with Mn or Oxyrase^{TM}, which reduces dissolved
101 oxygen. Altogether, our results indicate that the Ccn sRNAs prevents *S. pneumoniae* Zn
102 intoxication by reducing the intracellular abundance of free Zn, which in turn increases its

103 resistance to oxidative stress under aerobic growth condition as the result of an increase in the
104 amount of active superoxide dismutase A (SodA).
105
106 **RESULTS**
107 **The Ccn sRNAs are important for *S. pneumoniae* pathogenesis.** Work from a prior study (*12*)
108 indicated that deletion of one of the five Ccn sRNA genes (*ccnE*) reduced *S. pneumoniae* serotype
109 4 strain TIGR4 virulence in a murine invasive pneumoniae model. In that study, the authors also
110 discovered by Tn-seq that transposon insertions in *ccnE* reduced *S. pneumoniae* strain TIGR4
111 fitness in murine lungs, whereas transposon insertions in *ccnA* had no significant impact on its
112 fitness in the murine lung, nasopharynx, or blood. To determine the contribution of the Ccn sRNAs
113 to the virulence of the *S. pneumoniae* serotype 2 strain D39 in a murine invasive pneumonia
114 model, we initially made single deletions of *ccnA*, *ccnB*, *ccnC, ccnD*, or *ccnE* and a quintuple
115 deletion of all five *ccn* genes in a strain background harboring the *rpsL1* allele (IU1781). Next, we
116 evaluated the growth of these strains in BHI broth at 37ºC in an atmosphere of 5% CO_2. Neither
117 deletion of any single Ccn sRNA gene or all five of them had any significant effect on growth rate,
118 although the growth yield of the Δ*ccnE* strain was slightly reduced (Figs. 1A, S1A, and S1C). We
119 then determined the consequence of these deletions on *S. pneumoniae* pathogenicity in a murine
120 invasive pneumonia model (see Materials and Methods). While removal of any single *ccn* gene
121 had no significant impact on its virulence in mice (Fig. S2), deletion of all five *ccn* genes attenuated
122 *S. pneumoniae* strain D39 pathogenicity increasing median survival time from 43 h to 67 h (Fig.
123 2A).
124 To confirm that the *ccn* genes are generally important for *S. pneumoniae* virulence and is not
125 an attribute specific to strain D39, we also deleted all five *ccn* genes from a serotype 4 TIGR4
126 strain harboring the *rpsL1* allele (NRD10220) and measured the impact of these deletions on its
127 growth and virulence using the same murine invasive pneumonia model. As shown in Fig. 1D,
128 deletion of all five *ccn* genes did have an effect on growth rate of *S. pneumoniae* TIGR4 in BHI

129 broth incubated at 37°C with an atmosphere of 5% CO_2. To validate the effect of the *ccnABCDE*
130 deletion on *S. pneumoniae* TIGR4 growth, we reconstructed the quintuplet deletion strain from
131 scratch, but this time we subsequently replaced the mutant *rpsL* allele conferring streptomycin
132 resistance that aided in construction of the unmarked deletions of the *ccn* genes back to the wild
133 type *rpsL* allele. Next, we tested the growth of that strain and its parental *ccn*$^+$ TIGR4 strain in BHI
134 broth at 37°C under an atmosphere of 5% CO_2. Again, we saw a substantial reduction in growth
135 rate when all five *ccn* genes were deleted (Fig. S3A). The *ccnABCDE* deletion also resulted in a
136 marked attenuation of *S. pneumoniae* TIGR4 virulence increasing the survival rate of ICR outbred
137 mice from 0% to 50% (Fig. 2B). Two of the mice that survived infection with the TIGR4
138 Δ*ccnABCDE* strain had no detectable bacteria in the blood and the other two mice had 1,000 and
139 2,750 CFUs per mL of blood, respectively, which was far below 10^7 bacteria found in moribund
140 mice that were infected with the *ccn*$^+$ parent strain. Our results show that the *ccn* genes are
141 important for *S. pneumoniae* pathogenesis.
142
143 **The Ccn sRNAs impact expression of Zn and Mn-related genes.** To discover a basis for the
144 defect in *S. pneumoniae* virulence caused by the deletion of the five *ccn* genes, we compared
145 global gene expression by high throughput RNA-sequencing (RNA-seq) between *S. pneumoniae*
146 strain D39 or TIGR4 and the derived Δ*ccnABCDE* mutant strains grown to exponential phase
147 (OD_{620} between 0.15 and 0.2) in BHI broth at 37°C in an atmosphere of 5% CO_2. In the *S.*
148 *pneumoniae* D39 strain background, the *ccnABCDE* deletion resulted in down-regulation of 3
149 genes and up-regulation of 113 genes by 2-fold or more ($P_{adj} < 0.05$) (Table S3). In contrast,
150 deletion of the *ccn* genes from the TIGR4 strain resulted in down-regulation of 25 genes and up-
151 regulation of 97 genes by 2-fold or greater ($P_{adj} < 0.05$) (Table S4). 37 genes were up-regulated
152 by 2-fold ($P_{adj}<0.05$) in the *ccnABCDE* deletion strain in both the D39 and TIGR4 backgrounds
153 (Table 1); among these differentially expressed genes were iron uptake system genes (*piuB*,

154 *piuC*, *piuD*, and *piuA*), a Zn-responsive ECF (energy-coupling factor) transport gene
155 SPD_1267/SP_1438, and *czcD* encoding a Zn/Cd exporter that provides Zn and Cd resistance.
156 To validate our RNA-seq data, we first measured abundance of *piuB*, *spd_1267*, and *czcD*
157 transcripts in RNA samples isolated for the RNA-seq experiment from *S. pneumoniae* strain D39
158 and derived Δ*ccnABCDE* strain by reverse transcriptase droplet digital PCR (RT-ddPCR).
159 Consistent with our RNA-seq data the *piuB, spd_1267,* and *czcD* transcripts were up-regulated
160 by 3.5, 10.5, and 1.9-fold respectively in the Δ*ccnABCDE* strain compared to its parental D39
161 strain grown in BHI broth (Fig. 3A, B, and C). Using RT-ddPCR analysis of the RNA samples
162 isolated from exponential cultures of *S. pneumoniae* TIGR4 and derived Δ*ccnABCDE* mutant
163 strain grown in BHI broth at 37°C under an atmosphere of 5% CO_2, we also observed a 2.5-fold
164 increase in the abundance of the *czcD* mRNA in the *ccn* mutant as compared to its parental strain
165 (Fig. 3E). Altogether, these data suggested to us that removal of the *ccn* genes from *S.*
166 *pneumoniae* was leading to an increase in the intracellular free Zn concentration relative to Mn,
167 and to cope with this stress, the *ccn* mutant strain was increasing expression of the CzcD Zn
168 exporter.
169

170 **Table 1: Genes significantly, differentially expressed between a Δ*ccnABCDE* and *ccn*$^{+}$**
171 **strain in both the *S. pneumoniae* D39 and TIGR4 background during exponential growth**
172 **in BHI broth[a]**

D39 locus tag	Gene	Known or predicted function	D39 fold change	TIGR4 fold change
SPD_0025		tRNA-specific adenosine-34 deaminase	84.3	144
SPD_0027	*dut*	deoxyuridine 5'-triphosphate nucleotidohydrolase	3.52	4.39
SPD_0028		hypothetical protein	3.80	3.40
SPD_0029	*radA*	DNA repair protein	3.55	2.80
SPD_0090		galactose ABC transport protein	2.09	2.00
SPD_0104		aggregation-promoting factor	2.69	2.27
SPD_0222	*gpmB1*	phosphoglycerate mutase family protein	25.0	22.9
SPD_0243	*uppS*	undecaprenyl diphosphate synthase	5.97	4.42
SPD_0244	*cdsA*	phosphatidate cytidylyltransferase	5.50	4.49

SPD_0245	*eep*	intramembrane protease	5.57	4.19
SPD_0246	*proS*	prolyl-tRNA synthetase	5.91	4.68
SPD_0247	*bglA*	6-phospho-β-glucosidase	3.57	3.35
SPD_0308	*clpL*	ATP-dependent protease subunit	13.7	2.71
SPD_0460	*dnaK*	protein chaperone	3.97	2.01
SPD_0501	*licT*	β-glucoside operon antiterminator	2.91	4.77
SPD_0502	*bglF*	β-glucoside PTS transporter subunit	3.07	5.65
SPD_0503	*bglA-2*	6-phospho- β-glucosidase	2.57	4.79
SPD_0615	*glnH3*	degenerate glutamine ABC transporter subunit	11.6	4.05
SPD_0616	*glnQ3*	glutamine ABC transporter subunit	8.90	3.07
SPD_0617	*glnP3b*	glutamine ABC transporter subunit	11.1	3.63
SPD_0618	*glnP3a*	glutamine ABC transporter subunit	11.8	2.98
SPD_0775		acetyltransferase	3.29	2.71
SPD_1045		degenerate DUF3884 domain protein	4.73	3.16
SPD_1046	*lacG-2*	6-phospho-β-galactosidase	3.56	2.92
SPD_1267		ECF transporter subunit	11.1	2.14
SPD_1638	*czcD*	Cd/Zn exporter	2.69	2.66
SPD_1649	*piuB*	Fe uptake transporter subunit	5.13	2.43
SPD_1650	*piuC*	Fe uptake transporter subunit	4.45	2.01
SPD_1651	*piuD*	Fe uptake transporter subunit	4.22	2.15
SPD_1652	*piuA*	Fe uptake transporter subunit	4.38	2.25
SPD_1748	*pneA2*	lantibiotic peptide	2.19	2.16
SPD_1749	*lanM*	lanthionine biosynthesis protein	2.49	2.29
SPD_1750	*wrbA*	FAD-dependent flavoprotein	3.00	2.69
SPD_1751		hypothetical protein	2.56	3.16
SPD_1752	*clyB*	toxin secretion ABC transporter	3.58	3.22
SPD_1753		epidermin leader peptide processing serine protease	2.44	2.87
SPD_1932	*malP*	malodextrin phosphorylase	2.58	2.58

[a]RNA extraction and mRNA-seq analyses were performed as described in *Materials and Methods*. RNA was prepared from cultures of strains IU1781 (D39 *rpsL1*), NRD10176 (D39 *rpsL1* Δ*ccnABCDE*), NRD10220 (TIGR4 *rpsL1*), and NRD10266 (TIGR4 *rpsL1* Δ*ccnABCDE*) (Table S1 and S2). Fold changes (2.0-fold cut-off) and adjusted P-values (Pval <0.05) are based on three independent biological replicates.

Absence of the *ccn* genes causes S*. pneumoniae* to become hypersensitive to Zn. If the absence of the *ccn* genes from *S. pneumoniae* leads to an imbalance of transition metals with higher intracellular levels of free Zn relative to Mn, then we would expect that increasing the

183 concentration of Zn present in the medium would disproportionately impair the growth of the
184 Δ*ccnABCDE* mutant relative to the isogenic *ccn*$^+$ strain. Previous studies have indicated that
185 Becton-Dickinson (BD) BHI broth typically contains ~20 μM Zn and 200 nM Mn (*20, 21*). We first
186 compared growth of strain D39 and derived Δ*ccnA*, Δ*ccnB*, Δ*ccnC*, Δ*ccnD*, Δ*ccnE*, and
187 Δ*ccnABCDE* strains in BHI broth alone or supplemented with 0.2 mM Zn at 37°C under an
188 atmosphere of 5% CO_2. No significant difference was observed in growth rate between strain D39
189 and derived Δ*ccnA*, Δ*ccnB*, Δ*ccnC*, and Δ*ccnD* mutant strains in BHI in the presence or absence
190 of 0.2 mM added Zn (Fig. S1), although the growth yield for the *ccnE* mutant was lower in BHI in
191 the presence and absence of Zn. As noted above, growth of strain D39 and the derived
192 Δ*ccnABCDE* mutant was similar in BHI broth alone (Fig. 1A.)

193 In contrast, the absence of all five *ccn* genes led to an obvious impairment in growth rate in
194 BHI supplemented with 0.2 mM Zn (Fig. 1B) This growth deficiency relative to the *ccn*$^+$ parental
195 strain was also observed for the Δ*ccnABCDE* strain when Zn was increased in BHI broth to 0.4
196 mM (Fig. 1C). Consistently, addition of Zn at 0.4 mM severely reduced the growth rate of the *ccn*$^+$
197 D39 strain. Reintroduction of *ccnC* and *ccnD* expressed from their native promoters at ectopic
198 loci partially ameliorated the growth defect of the Δ*ccnABCDE* mutant strain in BHI supplemented
199 with 0.2 mM or 0.4 mM Zn, whereas insertion of copies of *ccnA, ccnB*, and *ccnD* with their native
200 promoter at the *bgaA* and CEP loci completely corrected the growth deficiency of this quintuple
201 *ccn* mutant (Figs. 1B and 1C) under these growth conditions. To verify that the Zn hypersensitivity
202 caused by the deletion of all five *ccn* genes was not specific to the serotype 2 strain D39, we also
203 tested the effect of the quintuple *ccn* deletion on the growth of the serotype 4 TIGR4 strain in BHI
204 broth supplemented with Zn. Consistent with our results observed for strain D39, deletion of the
205 Ccn sRNA genes from TIGR4 led to a growth impairment in BHI when Zn was added at a final
206 concentration of 0.2 or 0.4 mM (Figs. 1D-F and S3). Curiously, Zn at the highest concentration

207 used had less of an effect on TIGR4 growth than it did on the D39 strain. Overall, these results
208 indicate that Ccn sRNAs promote *S. pneumoniae* Zn tolerance.
209
210 **In the absence of the Ccn sRNAs, *S. pneumoniae* accumulates bioavailable Zn.** *S.*
211 *pneumoniae* is a Mn-centric bacteria encoding several Mn-requiring enzymes including
212 superoxide dismutase (SodA), a capsule regulatory kinase (CpsB), phosphoglucomutase (Pgm),
213 phosphopentomutase (DeoB), a cell division regulating phosphatase (PhpP), an aerobic
214 ribonucleotide reductase (NrdEF), pyruvate kinase (PyK), and lactate dehydrogenase (Ldh). Mis-
215 metalation of these Mn-dependent enzymes by Zn, which inhibits their enzymatic activity (*22, 23*),
216 can occur when the internal ratio of bioavailable Zn-to-Mn is high. Additionally, the substrate
217 binding component of the PsaBCA Mn ATP binding cassette (ABC) type transporter, the only
218 known Mn importer in *S. pneumoniae*, has been shown to bind Zn tightly, blocking Mn uptake (*20,*
219 *24*). Our RNA-seq and RT-ddPCR data above indicated that expression of the CzcD Zinc
220 exporter, which is expressed in response to high levels of free, or bioavailable, Zn relative to Mn
221 (*25, 26*), is up-regulated in *S. pneumoniae* strains lacking the *ccn* genes (Fig. 3C and E). Based
222 on these results and the published data mentioned above, we hypothesized that Zn-
223 hypersensitivity caused by the removal of all five *ccn* genes from the *S. pneumoniae* genome is
224 due to an increase in free Zn concentration relative to Mn. If this postulate is correct, then the Zn-
225 dependent growth inhibition that occurs when the *S. pneumoniae* Δ*ccnABCDE* mutant strain is
226 grown in BHI broth supplemented with 0.2 mM Zn should be rescued by inclusion of an equimolar
227 amount of Mn into the medium. As shown in Fig. 4, the growth impairment of the Δ*ccnABCDE*
228 mutant of *S. pneumoniae* D39 or TIGR4 strain in BHI broth with 0.2 mM Zn is cured by addition
229 of 0.2 mM Mn consistent with our model.
230 To directly test whether or not the levels of transition metals are perturbed in strains lacking
231 the *ccn* genes, we measured total cell-associated transition metals in *S. pneumoniae* strain D39,

232 derived Δ*ccnABCDE* mutant, and the Δ*ccnABCDE* strain complemented with *ccnA*, *ccnB*, and
233 *ccnD* grown in BHI broth or the chemically defined C medium by inductively coupled plasma-mass
234 spectrometry (ICP-MS). During exponential growth (OD_{620} of ~0.2) in BHI broth alone or
235 supplemented with 0.2 mM Zn, there was no significant difference in total cell-associated Zn
236 among these strains (Fig. 5A and B and Table 2). However, it remains possible that there was a
237 difference in the amount of bioavailable, or unbound, Zn as our ICP-MS based approach
238 measures the total amount of cell associated metals and does not discriminate between protein-
239 bound vs unbound metals.

240 Since we were unable to detect a difference in Zn or Mn content among the *S. pneumoniae*
241 strain D39 strain, Δ*ccnABCDE* mutant, and derived strain complemented with *ccnA, ccnB*, and
242 *ccnD* in BHI broth, we then assessed their abundance when these strains were grown in a defined
243 liquid medium (C-medium). Similar to what was observed in BHI broth supplemented with Zn, we
244 found that Δ*ccnABCDE* mutant had a slower growth rate, or longer doubling time, than its parental
245 *ccn*$^+$ *S. pneumoniae* D39 strain in C-medium supplemented with 0.2 mM $ZnSO_4$ (65 min vs 56
246 min), but not in C-medium alone (47 min vs 42 min) as shown in Fig. S4. Next, we measured total
247 cell-associated Zn and Mn of the aforementioned strains under these growth conditions, and we
248 observed a statistically significant difference ($P < 0.05$) in the median Zn abundance between the
249 *S. pneumoniae* strain D39 and derived Δ*ccnABCDE* mutant grown in C-medium alone (183%
250 increase) or supplemented with Zn (144% increase) (Fig. 5C and 5D and Table 2). No statistically
251 significant difference in total cell-associated Mn was observed between *S. pneumoniae* strain D39
252 and derived Δ*ccnABCDE* mutant under any of the tested growth conditions (Fig. 5B and 5D and
253 Table 2). Thus, our evidence that Mn supplementation eliminated the growth deficiency of the
254 *ccn*$^-$ strain caused by excess Zn (Fig. 4), that there was increased expression of *czcD* encoding
255 a Zn exporter when the *ccn* genes were removed from *S. pneumoniae* strains D39 and TIGR4
256 (Figs. 3C and 3E and Tables 1, S3, and S4), and that the amount of Zn associated with the

257 Δ*ccnABCDE* mutant strain was higher compared to the *ccn*$^+$ strain in C-medium (Fig. 5 and Table
258 2) suggest that the Ccn sRNAs are important for preserving Zn homeostasis in *S. pneumoniae*.
259
260 **Table 2: Total cell-associated Zn and Mn abundance of *S. pneumoniae* strain D39 and**
261 **derived Δ*ccnABCDE* strains grown in BHI broth or C medium alone or with Zn**
262 **supplementation[a]**

Strain	BHI		BHI + Zn		C		C + Zn	
	Zn	Mn	Zn	Mn	Zn	Mn	Zn	Mn
IU1781 (WT)	140 ±11 (6)	88 ±4.9 (6)	160 ±5 (5)	83 ±9.4 (5)	120 ±4 (8)	180 ±3 (8)	190 ±15 (5)	53 ±3 (5)
NRD10176 (Δccn)	150 ±12 (6)	100 ±4.4 (6)	160 ±13 (5)	91 ± 5.7 (5)	210 ±41 (5)	170 ±10 (5)	290 ±41 (5)	60 ±5 (5)
NRD10396 (Δccn//ccnA$^+$B$^+$D$^+$)	160 ±15 (6)	100 ±8.6 (6)	220 ±21 (6)	93 ± 6.1 (6)	170 ±17 (6)	170 ±12 (6)	320 ±66 (5)	65 ±6 (5)

263 [a]The indicated strains were cultured and ICP-MS analyses of metal abundance of cells harvested
264 from these cultures was performed as described in *Materials and Methods*. Shown are the mean
265 values of the Zn and Mn abundance normalized to protein levels (ng/mg of protein) followed by
266 the standard error of the mean. Number of biological replicates is indicated in parentheses. The
267 median values of Zn and Mn abundance from these experiments are shown in Fig. 5.
268
269 **Oxidative stress due to reduced levels of active superoxide dismutase A contributes to the**
270 **Zn hypersensitivity of the *S. pneumoniae* strain lacking the Ccn sRNAs.** To discover the

271 molecular basis for the Zn hypersensitivity caused by loss of the *ccn* genes, we turned to an RNA-
272 seq based approach. Briefly, we compared transcript abundance in RNA isolated from *S.*
273 *pneumoniae* strain D39 and derived Δ*ccnABCDE* strain grown to exponential phase (OD_{620} of
274 ~0.2) at 37°C under an atmosphere of 5% CO_2 in BHI broth supplemented with 0.2 mM Zn. Similar
275 to our RNA-seq experiments performed with these strains in the absence of Zn supplementation,
276 we observed a 2.3-fold increase in expression of the CzcD Zn exporter specifying mRNA and a
277 9.5-fold increase in the Spd_1267 Zn-responsive ECF-type transporter producing mRNA in the
278 Δ*ccnABCDE* mutant compared to its *ccn*$^+$ parent strain (Tables 3 and S5). Interestingly, we also
279 saw a 1.9-fold decrease ($P_{adj} = 1.81 \times 10^{-43}$) in expression of the *sodA* mRNA, encoding superoxide
280 dismutase A, in the Δ*ccnABCDE* mutant strain, which was just below our arbitrary two-fold cutoff
281 (Table S5). We subsequently measured the relative abundance of these transcripts by RT-ddPCR
282 and northern blot analysis (Figs. 3B, C, and D) and were able to confirm our RNA-seq results
283 indicating up-regulation of *spd_1267* and *czcD* mRNAs and down-regulation of the *sodA* mRNA
284 abundance when the *ccn* genes were deleted from *S. pneumoniae*. This result was intriguing to
285 us since a prior study found that Mn starvation of *S. pneumoniae* cells due to exposure to high
286 concentrations of Zn relative to Mn led to a reduction in the transcription of *sodA* and a reduction
287 in superoxide dismutase activity (*22*). Furthermore, Eijkelkamp *et* al discovered that deletion of
288 *sodA* had no significant impact on *S. pneumoniae* growth under Mn replete conditions, but was
289 vital for growth in media containing a high Zn-to-Mn ratio (*22*).
290

291 **Table 3: Genes significantly, differentially expressed between a *S. pneumoniae* D39 and**
292 **derived Δ*ccnABCDE* strain in both BHI alone or supplemented with Zn[a]**

D39 locus tag	Gene	Known or predicted function	Fold change (BHI)	Fold change (BHI+Zn)
SPD_0025		tRNA-specific adenosine-34 deaminase	84.3	49.0
SPD_0027	*dut*	deoxyuridine 5'-triphosphate nucleotidohydrolase	3.52	3.76

SPD_0028		hypothetical protein	3.80	3.02
SPD_0029	*radA*	DNA repair protein	3.55	2.95
SPD_0080	*pavB*	cell wall surface anchor family protein	6.69	6.32
SPD_0163		DNA binding protein	2.00	2.07
SPD_0222	*gpmB1*	phosphoglycerate mutase family protein	25.0	21.7
SPD_0243	*uppS*	undecaprenyl diphosphate synthase	5.97	7.61
SPD_0244	*cdsA*	phosphatidate cytidylyltransferase	5.50	7.77
SPD_0245	*eep*	intramembrane protease	5.57	8.59
SPD_0246	*proS*	prolyl-tRNA synthetase	5.91	9.65
SPD_0247	*bglA*	6-phospho-β-glucosidase	3.57	4.73
SPD_0277	*bglA-1*	6-phospho-β-glucosidase	3.53	2.73
SPD_0279	*celB*	cellobiose PTS transporter subunit	5.05	2.97
SPD_0308	*clpL*	ATP-dependent protease subunit	13.7	9.55
SPD_0350	*vraT*	cell wall-active antibiotic response protein	2.19	2.62
SPD_0351	*vraS*	two-component system histidine kinase	2.29	2.74
SPD_0352	*vraR*	two-component system response regulator	2.31	2.70
SPD_0353	*alkD*	degenerate DNA alkylation repair enzyme	2.11	2.67
SPD_0354	*alkD*	degenerate DNA alkylation repair enzyme	2.37	2.69
SPD_0458	*hrcA*	heat inducible transcription repressor	3.62	3.69
SPD_0459	*grpE*	heat shock protein	3.77	3.87
SPD_0460	*dnaK*	protein chaperone	3.97	3.82
SPD_0461	*dnaJ*	protein chaperone	3.50	3.52
SPD_0474	*blpZ*	immunity protein	2.40	2.05
SPD_0501	*licT*	β-glucoside operon antiterminator	2.91	5.26
SPD_0502	*bglF*	β-glucoside PTS transporter subunit	3.07	4.65
SPD_0503	*bglA-2*	6-phospho- β-glucosidase	2.57	3.75
SPD_0537		putative Zn-dependent protease	2.07	2.21
SPD_0615	*glnH3*	degenerate glutamine ABC transporter subunit	11.6	18.0
SPD_0616	*glnQ3*	glutamine ABC transporter subunit	8.90	16.8
SPD_0617	*glnP3b*	glutamine ABC transporter subunit	11.1	15.8
SPD_0618	*glnP3a*	glutamine ABC transporter subunit	11.8	15.1
SPD_0681		hypothetical protein	2.82	5.45
SPD_0701	*ciaR*	two-component response regulator	2.72	2.56
SPD_0702	*ciaH*	two-component histidine kinase	2.80	3.01
SPD_0775		acetyltransferase	3.29	3.61
SPD_0803		putative phage shock protein C		
SPD_0804		ABC transporter ATP-binding protein	2.28	3.01
SPD_0805		ABC transporter permease protein	2.43	3.15
SPD_0913		extracellular protein	3.39	3.31
SPD_0938		degenerate TN5252 relaxase	9.35	5.06
SPD_0940	*rrfD*	UDP-N-acetyl-D-mannosaminouronic acid dehydrogenase.	3.95	5.31
SPD_0942		hypothetical protein	2.25	2.41
SPD_0943		hypothetical proein	2.41	2.43
SPD_0944		nodulation protein L	2.24	2.38
SPD_0946		hypothetical protein	2.16	3.27
SPD_0947		hypothetical protein	2.69	3.97
SPD_0948	*nikS*	nikkomycin biosynthesis protein	3.73	4.29

SPD_0949		N-acetylneuraminate synthase	2.38	4.85
SPD_0950	*mefE*	macrolide ABCE transporter subunit	2.44	3.99
SPD_1045		degenerate DUF3884 domain protein	4.73	6.81
SPD_1046	*lacG-2*	6-phospho-b-galactosidase	3.56	7.28
SPD_1047	*lacE-2*	lactose PTS transporter subunit	4.21	6.33
SPD_1049	*lacT*	β-glucoside *bgl* operon antiterminator	3.23	3.48
SPD_1114		hypothetical protein	13.5	5.37
SPD_1267		ECF transporter subunit	11.1	9.53
SPD_1297	*pdxS*	pyridoxal 5'-phosphate synthase	2.02	2.04
SPD_1506	*axe1*	acetyl xylan esterase 1	3.62	2.68
SPD_1615		degenerate hypothetical protein	4.02	2.09
SPD_1638	*czcD*	Cd/Zn exporter	2.69	2.33
SPD_1709	*groL*	HSP60 family chaperone	2.58	2.38
SPD_1710	*groES*	HSP60 family chaperone	2.25	2.31
SPD_1716		hypothetical protein	2.56	5.62
SPD_1717		membrane protein	2.40	5.22
SPD_1718		LytR/AlgR family response regulator	2.44	4.58
SPD_1746		hypothetical protein	2.96	4.25
SPD_1747	*pneA1*	lantibiotic peptide	2.02	4.29
SPD_1748	*pneA2*	lantibiotic peptide	2.19	4.60
SPD_1749	*lanM*	lanthionine biosynthesis protein	2.49	2.37
SPD_1750	*wrbA*	FAD-dependent flavoprotein	3.00	2.85
SPD_1751		hypothetical protein	2.56	4.07
SPD_1752	*clyB*	toxin secretion ABC transporter	3.58	4.02
SPD_1753		epidermin leader peptide processing serine protease	2.44	3.00
SPD_1769		membrane protein	2.29	3.42
SPD_1932	*malP*	malodextrin phosphorylase	2.58	2.95
SPD_1933	*malQ*	4-α-glucanotransferase	2.76	2.77
SPD_1990		mannose PTS transporter subunit	2.01	13.8
SPD_1994	*fucA*	L-fuculose phosphate aldolase	2.35	8.69
SPD_2034	*comFC*	phosphororibosyltransferase domain protein	32.7	14.1
SPD_2035	*comFA*	DNA transporter ATPase	8.88	10.2
SPD_2068	*htrA*	serine protease	2.79	2.13
SPD_2069	*parB*	chromosome partitioning protein	3.04	2.88

[a]RNA extraction and mRNA-seq analyses were performed as described in *Materials and Methods*. RNA was prepared from cultures of strains IU1781 (D39 *rpsL1*) and NRD10176 (D39 *rpsL1* Δ*ccnABCDE*) grown to exponential phase in BHI alone or supplemented with 0.2 mM $ZnSO_4$ (Table S1 and S2). Fold changes (2.0-fold cut-off) and adjusted P-values (Pval <0.05) are based on three independent biological replicates.

300 To initially examine whether the growth deficiency of the Δ*ccnABCDE* mutant relative to the
301 *ccn*$^+$ D39 strain was due in part to oxidative stress, we evaluated the impact of addition of
302 Oxyrase™, an enzyme mixture that removes molecular oxygen by reducing it to water, on the
303 growth of these strains in BHI broth alone or supplemented with 0.2 mM or 0.4 mM Zn (Fig 6A, B,
304 and C) under an atmosphere of 5% CO_2. Once again, we observed that deletion of *ccnA*, *ccnB*,
305 *ccnC*, *ccnD*, and *ccnE* from *S. pneumoniae* strain D39 had no significant impact on growth in BHI
306 alone. However, under these growth conditions, the addition of Oxyrase™ reduced the growth
307 rate of both the *ccn*$^+$ and ccn$^-$ strains to a similar extent (Fig. 6A). As we anticipated, addition of
308 Oxyrase™ to BHI supplemented with Zn (0.2 mM) improved the growth rate of the Δ*ccnABCDE*
309 strain to that observed for the *ccn*$^+$ D39 parent strain (Fig. 6B). Interestingly, addition of Oxyrase™
310 improved the growth rate of both strains in BHI with 0.4 mM Zn and eliminated any growth
311 differences between them (Fig. 6C). Finally, we examined the contribution of *sodA* to the growth
312 of *S. pneumoniae* D39 and derived Δ*ccnABCDE* mutant strain. In BHI broth alone or
313 supplemented with 0.2 mM Zn, deletion of *sodA* reduced the growth rate of the *ccn*$^+$ strain, but
314 did not result in a significant reduction in growth rate of the Δ*ccnABCDE* mutant strain (Fig. 7).
315 Based on these results, we concluded that the amount of functional SodA was negligible in the
316 *S. pneumoniae* strain lacking the Ccn sRNAs and thus, deleting *sodA* did not significantly impact
317 its growth, whereas this deletion did impair growth of the isogenic *ccn*$^+$ strain.
318

319 **DISCUSSION**

320 High density Tn-seq experiments performed more than a decade ago revealed that sRNAs
321 play a crucial role in regulating *S. pneumoniae* virulence including its ability to colonize the blood,
322 nasopharynx, and lungs of its host (*12*). While this discovery in itself may not be surprising, it is
323 astonishing that very little progress has been made towards understanding the functions of these
324 sRNAs given their importance in governing *S. pneumoniae* pathogenesis. Here, we investigated

325 the contribution of the five homologous Ccn sRNAs to *S. pneumoniae* pathogenesis and gene
326 regulation. Not only have we confirmed their crucial role in pneumococcal disease progression
327 (Fig. 2), but also discovered their extensive functions in regulating gene expression and Zn
328 resistance. Specifically, we found that exposure to relatively high, yet host-relevant, Zn
329 concentrations (0.2 mM) disproportionally inhibited *S. pneumoniae* growth in BHI broth (Fig 1, 4,
330 6, and 7) and modestly increased total cell-associated Zn levels (Fig. 5 and Table 2) of *S.*
331 *pneumoniae* strains lacking genes for the five Ccn sRNAs grown in C-medium alone or
332 supplemented with 0.2 mM $ZnS0_4$. While we were unable to detect by ICP-MS a statistically
333 significant difference in Zn content between *S. pneumoniae* and derived Δ*ccnABCDE* mutant
334 strain grown in BHI broth alone or supplemented with Zn, we suspect that loss of the Ccn sRNA
335 genes does increase the amount of bioavailable Zn in *S. pneumoniae* under these growth
336 conditions since increased *czcD* expression is a sensitive indicator of high levels of bioavailable
337 Zn inside of cells (*25*). The Zn-dependent growth inhibition caused the *ccnABCDE* deletion was
338 completely alleviated by addition of Mn (Fig. 4) or Oxyrase™ (Fig. 6), which removes molecular
339 oxygen by reducing it to water. Furthermore, deletion of *sodA*, encoding the Mn-dependent
340 superoxide dismutase A, from *S. pneumoniae* resulted in a Zn-dependent growth inhibition;
341 however, the same deletion had no impact on the growth of the Δ*ccnABCDE* strain (Fig. 7).
342 Altogether, these results indicate that the Ccn sRNAs promote Zn homeostasis resulting in an
343 increased abundance of active SodA, which improves the growth of *S. pneumoniae* in a Zn-rich
344 environment due to greater protection from damaging reactive oxygen species.

345 How do the Ccn sRNAs prevent *S. pneumoniae* from accumulating bioavailable Zn^{2+} cations
346 relative to Mn^{2+}? The Ccn sRNAs could preclude a Zn buildup by (1) promoting expression of a
347 Zn exporter, (2) negatively regulating expression of a Zn importer, or (3) increasing production of
348 an intracellular protein or other factor that effectively chelates Zn. As mentioned already, CzcD is
349 the main Zn exporter in *S. pneumoniae* and is essential for Zn resistance (*27*). In contrast, the

350 Adc system is important for Zn uptake, but supplementation with Zn is able to bypass the
351 requirement for this transporter indicating that other low-affinity Zn importers exist in *S.*
352 *pneumoniae* (*28-30)*. Our global analysis of gene expression in *S. pneumoniae* D39 or TIGR4
353 and derived Δ*ccnABCDE* mutant strain revealed that *czcD* expression increased when the *ccn*
354 genes were removed, whereas no significant difference in expression of any of the *adc* genes
355 was observed. Thus, while we are not able to rule out the possibility that the Ccn sRNAs regulate
356 expression of an uncharacterized transporter capable of translocating Zn, our results indicate that
357 the Zn sensitivity of the Δ*ccnABCDE* mutant strain is not due to reduced expression of *czcD* or
358 up-regulation of the Adc system. While it also remains possible that the Ccn sRNAs regulate
359 production of an unknown factor that chelates or chaperones intracellular Zn, we did not observe
360 a reduction in the expression of any *known* Zn-binding proteins in the *ccn* mutant relative to its
361 parental *ccn*$^+$ *S. pneumoniae* D39 or TIGR4 strain via RNA-seq (Tables 1, 3, S3, S4, and S5).
362 Even though, we did not observe a statistically significant decrease in total cell-associated Mn
363 in the Δ*ccnABCDE* mutant relative to its parental *S. pneumoniae* D39 strain, we still wondered
364 whether or not loss of the Ccn sRNAs caused Zn sensitivity due to reduced uptake or increased
365 export of Mn, since the ICP-MS based approach that we utilized measures total, not bioavailable
366 metal abundance. The main Mn exporter of *S. pneumoniae* is MntE, as deletion of the encoding
367 gene leads to accumulation of total cell associated Mn (*21, 31*). MgtA, designated as a Ca efflux
368 protein, appears to also export Mn, but has a very limited role in this process (*32*). Neither MntE
369 or MgtA were up-regulated in either *S. pneumoniae* strain D39 or TIGR4 when the *ccn* genes
370 were deleted (Tables S3 S4, and S5) making it unlikely that the Ccn sRNAs increase intracellular
371 Mn levels by down-regulating expression of these Mn exporter genes. Additionally, we were
372 unable to identify strong Ccn sRNA binding sites in the translation initiation region of *mntE* or
373 *mgtA*, which suggests that these sRNAs do not directly regulate translation of these transcripts.
374 Finally, if the Ccn sRNAs increase total cell-associated Mn levels by down-regulating MntE

375 expression, then we would expect that deletion of *mntE* would suppress the Zn hypersensitivity
376 of the *S. pneumoniae* Δ*ccnABCDE* mutant; however, this did not occur (Fig S5A and C).

377 An alternative possibility is that the Ccn sRNAs promote Mn uptake by positively regulating
378 expression of the *psaBCA* operon encoding the only known Mn importer in *S. pneumoniae* (*29,*
379 *33*). Localized to the inner membrane, PsaB is the ATP binding component whereas PsaC is the
380 permease of this ABC-type transporter. PsaA, the substrate binding component, is located in the
381 periplasm, where it binds Mn. Once again, in our RNA-seq experiments, we did not observe a
382 decrease in expression of the *psaBCA* operon when the *ccn* genes were deleted from *S.*
383 *pneumoniae* strain D39 or TIGR4 (Tables S3, S4, and S5) indicating that the Ccn sRNAs do not
384 positively regulate expression of this Mn importer. Furthermore, if this was the case, then we
385 would expect that deletion of *psaR* encoding the repressor of the *psaBCA* operon (*34, 35*) might
386 suppress the Zn-dependent growth inhibition of the *S. pneumoniae* Δ*ccnABCDE* mutant;
387 however, we did not observe this (Fig. S5B and D).

388 In summary, we show that Ccn sRNAs play a key role in controlling the ability of *S.*
389 *pneumoniae* to cause invasive pneumoniae (Fig. 2) and resist Zn intoxication (Fig. 3). Our results
390 indicate that the reduced growth of *S. pneumoniae* in the presence of excess, but physiologically
391 relevant Zn concentrations caused by loss of the Ccn sRNA is due to an increase in oxidative
392 stress (Figs. 6 and 7). Our work suggests that there are likely additional, uncharacterized factors
393 that modulate bioavailable Zn abundance in pneumococcus.

394

395 **MATERIALS AND METHODS**

396 **Bacterial strains and growth conditions.** Bacterial strains used in this study were derived
397 from encapsulated *S. pneumoniae* serotype 2 strain D39W (*14*) and TIGR4 and are listed in Table
398 S1. Strains were grown on plates containing trypticase soy agar II (modified; Becton-Dickinson
399 [BD]) and 5% (vol/vol) defribrinated sheep blood (TSAII BA) at 37°C in an atmosphere of 5% CO_2,

400 and liquid cultures were statically grown in BD brain heart infusion (BHI) broth or C-medium (*36*)
401 at 37°C in an atmosphere of 5% CO_2. C-medium was prepared as described by Lacks and
402 Hotchkiss, but water was added in place of yeast extract. Bacteria were inoculated into BHI broth
403 from frozen cultures or single, isolated colonies. For overnight cultures, strains were first
404 inoculated into a 17-mm-diameter polystyrene plastic tube containing 5 mL of BHI broth and then
405 serially diluted by 100-fold into four tubes; these cultures were then grown for 10 to 16 h. Cultures
406 with an optical density at 620 nm (OD_{620}) of 0.1 to 0.4 were diluted to a starting OD_{620} between
407 0.002 and 0.005 in 5 mL of BHI broth in 16-mm glass tubes. For growth in C-medium, 2 mL of
408 overnight cultures grown in BHI with an OD_{620} of 0.1 to 0.4 were spun down at 21,000 x *g* for 2.5
409 min at room temperature. The supernatant was removed, and the pellet was washed with 1.0 mL
410 of C-medium. The solution was vortexed to resuspend the pellet and spun again at 21,000 x *g* for
411 2.5 min at room temperature. The supernatant was removed and the pellet was resuspended in
412 4.0 mL of C-medium. OD_{620} was used to determine how much culture to add to 5.0 mL of C-
413 medium in 16 mm glass tubes to begin growth at OD_{620} = 0.002. Growth was monitored by
414 measuring OD_{620} using a Genesys 30 visible spectrophotometer (ThermoFisher Scientific). For
415 antibiotic selections, TSAII BA plates and BHI cultures were supplemented with 250 µg kanamycin
416 per mL, 150 µg streptomycin per mL, or 0.3 µg erythromycin per mL.
417
418 **Construction and confirmation of mutants.** Mutant strains were constructed by
419 transformation of competent *S. pneumoniae* D39 and TIGR4 derived strains with linear PCR
420 amplicons as described previously (*37, 38*). DNA amplicons containing antibiotic resistance
421 markers were synthesized by overlapping fusion PCR using the primers listed in Table S2.
422 Competence was induced in *S. pneumoniae* D39 or TIGR4 derived cells with CSP-1 or CSP-2,
423 respectively, synthetic competence stimulatory peptide. Unmarked deletions of the target genes
424 were constructed using the kan^R-$rpsL^+$ (Janus cassette) allele replacement method as described
425 previously (*39*). In the first step, the Janus cassette containing $rpsL^+$ allele and a kanamycin

426 resistance gene was used to disrupt target genes in an *rpsL1* or *rpsLK56T* (Str^R) strain
427 background, and transformants were selected for kanamycin resistance and screened for
428 streptomycin sensitivity. In the second step, the Janus cassette was eliminated by replacement
429 with a PCR amplicon lacking antibiotic markers and the resulting transformants were selected for
430 streptomycin resistance and screened for kanamycin sensitivity. Freezer stocks were made of
431 each strain from single colonies isolated twice on TSAII BA plates containing antibiotics listed in
432 Table S1. All strains were validated by PCR amplification and sequencing.
433
434 **RNA extraction.** To isolate RNA, strains were grown in 30 mL of BHI starting at an OD_{620} =
435 0.002 in 50 mL conical tubes. RNA was extracted from exponentially growing cultures of IU1781
436 (D39), NRD10220 (TIGR4), and their derived isogenic mutants lacking all five *ccn* genes,
437 NRD10176 (D39 Δccn) and NRD10266 (TIGR4 Δccn), at $OD_{620} \approx 0.2$ using the FastRNA Pro Blue
438 Kit (MP Bio) according to the manufacturer's guidelines. Briefly, cells were collected by
439 centrifugation at 16,000 x g for 8 min at 4°C. Cell pellets were resuspended in 1 mL of RNApro™
440 solution (MP Bio) and processed five-times for 40 sec at 400 rpm in a BeadBug™ homogenizer
441 (Benchmark Scientific). Cell debris was removed by centrifugation at 16,000 x g for 5 min at 4°C.
442 After mixing 300 μL of chloroform with the supernatant, the aqueous and organic layers were
443 separated by centrifugation at 16,000 x g for 5 min at 4°C. RNA was precipitated with 500 μL of
444 ethanol at -80°C overnight. After collecting the precipitated RNA by centrifugation at 16,000 x g
445 for 15 min at 4°C, the pellet was washed once with 75% ethanol and suspend in DEPC-treated
446 water. The amount and purity of all RNA samples isolated were assessed by NanoDrop
447 spectroscopy (Thermo Fisher).
448
449 **Library preparation and mRNA-seq.** cDNA libraries were prepared from total RNA Azenta Life
450 Sciences. Briefly, total RNA was subjected to rRNA-depletion using the FastSelect 5S/16S/23S

451 rRNA depletion kit for bacteria. Libraries were the generated with NEBNext Ultra™ II Directional
452 RNA Library Prep Kit. 150 bp paired-end read sequencing was performed using an Illumina
453 HiSeq4000 sequencer.
454
455 **RNA-seq analysis.** The raw sequencing reads were quality and adapter trimmed using Cutadapt
456 version 4.1 with a minimum length of 18 nucleotides. The trimmed reads were then mapped on
457 the *Streptococcus pneumoniae* D39 (Genbank CP000410) genome using Bowtie2 (*40*). HTseq
458 version 2.0.2 was used to generate read counts for the genes (*41*). Differential gene expression
459 was identified using the program DESeq2 with default parameters (*42*). Primary data from the
460 mRNA-seq analyses were submitted to the NCBI Gene Expression Omnibus (GEO) and have
461 the accession number GSE246655.
462
463 **Reverse transcriptase-droplet digital PCR (RT-ddPCR) analysis.** RT-ddPCR was performed
464 as described previously (*43*). Isolated RNA was treated with DNase (TurboDNase, Ambion) as
465 per manufacturer's instructions. Next, RNA (1 μg) was reverse transcribed using Superscript III
466 reverse transcriptase (Invitrogen) with random hexamers. RT and No RT control (NRT) sample
467 were utilized. These samples were diluted $1:10^1$, $1:10^2$, $1:10^3$, or $1:10^6$. Then, 2 μL of each diluted
468 RT and NRT sample was added to a 22 μL reaction mixture containing 11 μL of QX200™ ddPCR
469 ™ Evagreen Supermix (Bio-Rad) and 1.1 μL of each 2 μM ddPCR primers (Table S6). A single
470 no template control (NTC) was included for each ddPCR primer pair used. Reactions were
471 performed using at least three independent biological replicates. Droplets were generated using
472 the QX200 Automated Droplet Generator (Bio-Rad), and end-point PCR was carried out using a
473 C1000 Touch™ thermal cycler (Bio-Rad) following the manufacturer's instructions. Quantification
474 of PCR-positive and PCR-negative droplets in each reaction, which provides absolute
475 quantification of the target transcript, was performed using the QX200 Droplet Reader (Bio-Rad).

476 This data was analyzed with QuantaSoft software (Bio-Rad) to determine the concentration of
477 each target expressed as copies per µL. Transcript copies were normalized to *tuf* mRNA (internal
478 control) and fold changes of transcripts corresponding to target genes in different mutants relative
479 to the WT parent were calculated. Statistical analysis was performed using Student's t-test with
480 GraphPad Prism version 10.0.0.
481
482 **Northern blot analysis.** Northern blotting was conducted as previously described (*13*). Briefly,
483 3 µg of isolated RNA was fractionated on 10% polyacrylamide gels containing 7% urea by
484 electrophoresis at 55 V and subsequently, transferred to a Zeta-probe membrane (Bio-Rad) using
485 a Trans-Blot SD semidry transfer apparatus (Bio-rad) at 4 mA per cm^2 with a maximum of 400
486 mA for 50 min. RNA was then UV-crosslinked to the membrane with a Spectroline UV crosslinker
487 with the "optimal crosslink" setting. 5'-Biotinylated probes were hybridized to the membrane
488 overnight at 42°C in ULTRAhyb (Ambion) hybridization buffer. Blots were developed according to
489 the BrightStar BioDetect kit protocol (Ambion), imaged with the ChemiDoc MP imager (Bio-Rad),
490 and individual band intensities were quantified using Image Lab software version 5.2.1 (Bio-Rad).
491 Signal intensities for each transcript were normalized to that of 5S rRNA, which served as a
492 loading control. Graphs of normalized abundance of each transcript for three biological replicates
493 were produced using GraphPad Prism version 10.0.0.
494
495
496 **Inductively coupled plasma-mass spectrometry (ICP-MS) analysis.** ICP-MS sample
497 preparation was based on a previous publication (*44*), with some modifications. Metal-free
498 microfuge tubes were used throughout, and pipette tips were rinsed prior to use. Bacteria were
499 grown in BHI broth or C medium at 37°C with 5% CO_2 to OD_{620} = 0.2. Five mL of culture was
500 centrifuged for 10 min in pre-chilled tubes at 12,400 x *g* at 4°C, and cell pellets were resuspended
501 in 1.0 mL of chilled BHI supplemented with 1 mM nitrilotriacetic acid (Sigma-Aldrich) (pH 7.2).

502 Samples were centrifuged for 7 min at 16,100 x *g* at 4°C, and supernatants were removed. Pellets
503 were centrifuged for an additional 3 min in the same way, and residual supernatant was removed.
504 Cell pellets were washed twice with centrifugation in the same way with 1.0 mL of chilled PBS
505 lacking K^+ (130 mM NaCl, 8.8mM Na_2HPO_4, 1.2mM NaH_2PO_4, pH 7.0) that had been treated with
506 chelator. Chelated PBS was prepared by mixing with 1% (wt/vol) Chelex-100 (BioRad), which
507 was rotated overnight at 4°C and passed through a 0.22 µm Steriflip (MilliporeSigma) filter. Before
508 the last centrifugation in PBS, samples were split into two 0.475 mL aliquots for ICP-MS analysis
509 and protein quantification. After removal of supernatants, pellets for ICP-MS were dried for 15 h
510 at low heat in an evaporative centrifuge and stored at -80°C until being processed for ICP-MS
511 analysis. Pellets for protein determination were suspended in in 100 µL of lysis buffer (1% (wt/vol)
512 SDS [Sigma], 0.1% w/v Triton X-100 [Mallinckrodt]) and stored at -80°C. Protein amount was
513 determined by using the DC protein assay (BioRad). For ICP-MS analysis, dried samples were
514 resuspended in 400 µL of 30% trace metal grade HNO_3 (Sigma). Samples and a 30% HNO_3 blank
515 were heated at 95° C for 10 min with shaking at 500 rpm. Samples were then diluted 100-fold to
516 a final volume of 3.0 mL with 2.5% HNO_3 containing the Pure Plus Internal Standard Mix (100
517 ppb, PerkinElmer). Samples were analyzed using an Agilent 8800 QQQ ICP-MS operating with
518 hydrogen (^{55}Mn detection) or helium (^{66}Zn detection) as collision gases to remove possible
519 interferences. ^{45}Sc or ^{72}Ge were used as internal references. Zn^{2+} and Mn^{2+} amounts were
520 calculated from standard curves made with Pure Plus Multi-Element Calibration Standard 3 (0.5-
521 100ppb, PerkinElmer). Metals amounts detected in the 30% HNO_3 blank were subtracted from all
522 samples. Metal amounts in samples were normalized relative to total protein amounts in the
523 matched samples.
524
525 **Mouse models of infection:** All procedures were approved in advance by UTHealth Animal
526 Welfare Committee and carried out as previously described (*43*). Male ICR mice (21-24 g; Envigo)
527 were anaesthetized by inhaling 4 to 5 % isoflurane. A total of 8 mice were intranasally inoculated

528 with 10^7 CFU of a specific *S. pneumoniae* strain suspended in 50 μL of 1 X PBS prepared from
529 cultures grown in BHI broth at 37°C in an atmosphere of 5% CO_2 to $OD_{620} \approx 0.1$. Mice were
530 monitored visually at 4 to 8 h intervals, and isoflurane-anesthetized moribund mice were
531 euthanized by cardiac puncture-induced exsanguination followed by cervical dislocation. Kaplan-
532 Meir survival curves and log-rank tests were generated using GraphPad Prism 10.0.0 software.
533

534 **SUPPLEMENTAL MATERIALS**

535 Supplemental Materials are available for this article.
536

537 **ACKNOWLEDGEMENTS**

538 This work was supported by NIGMS grant T32GM131994 (to M.O.), NIGMS grant R35GM118157
539 (to D.P.G.), NIGMS grant R35GM131767 (to M.E.W.), McGovern Medical Startup funds, and
540 NIAID grant R21AI171771 (to N.R.D.).
541

542 **REFERENCES**

543 1. D. G. Mediati, S. Wu, W. Wu, J. J. Tree, Networks of Resistance: Small RNA Control of
544 Antibiotic Resistance. *Trends Genet* **37**, 35-45 (2021).
545 2. R. Ghandour, K. Papenfort, Small regulatory RNAs in *Vibrio cholerae*. *Microlife* **4**, uqad030
546 (2023).
547 3. K. Papenfort, S. Melamed, Small RNAs, Large Networks: Posttranscriptional Regulons in
548 Gram-Negative Bacteria. *Annual review of microbiology*, (2023).
549 4. J. Hor, G. Matera, J. Vogel, S. Gottesman, G. Storz, Trans-Acting Small RNAs and Their
550 Effects on Gene Expression in *Escherichia coli* and *Salmonella enterica*. *EcoSal Plus* **9**,
551 (2020).
552 5. C. Pourciau, Y. J. Lai, M. Gorelik, P. Babitzke, T. Romeo, Diverse Mechanisms and Circuitry
553 for Global Regulation by the RNA-Binding Protein CsrA. *Frontiers in Microbiology* **11**,
554 601352 (2020).
555 6. M. G. Jorgensen, J. S. Pettersen, B. H. Kallipolitis, sRNA-mediated control in bacteria: An
556 increasing diversity of regulatory mechanisms. *Biochim Biophys Acta Gene Regul Mech*
557 **1863**, 194504 (2020).
558 7. L. Bossi, N. Figueroa-Bossi, P. Bouloc, M. Boudvillain, Regulatory interplay between small
559 RNAs and transcription termination factor Rho. *Biochim Biophys Acta Gene Regul Mech*
560 **1863**, 194546 (2020).
561 8. F. Ponath, J. Hor, J. Vogel, An overview of gene regulation in bacteria by small RNAs
562 derived from mRNA 3' ends. *FEMS Microbiology Reviews* **46**, (2022).

563 9. G. B. D. L. R. I. Collaborators, Estimates of the global, regional, and national morbidity,
564 mortality, and aetiologies of lower respiratory infections in 195 countries, 1990-2016: a
565 systematic analysis for the Global Burden of Disease Study 2016. *Lancet Infect Dis* **18**,
566 1191-1210 (2018).
567 10. P. Acebo, A. J. Martin-Galiano, S. Navarro, A. Zaballos, M. Amblar, Identification of 88
568 regulatory small RNAs in the TIGR4 strain of the human pathogen *Streptococcus*
569 *pneumoniae*. *RNA* **18**, 530-546 (2012).
570 11. R. Kumar *et al.*, Identification of novel non-coding small RNAs from *Streptococcus*
571 *pneumoniae* TIGR4 using high-resolution genome tiling arrays. *BMC Genomics* **11**, 350
572 (2010).
573 12. B. Mann *et al.*, Control of virulence by small RNAs in *Streptococcus pneumoniae*. *PLoS*
574 *Pathogens* **8**, e1002788 (2012).
575 13. D. Sinha *et al.*, Redefining the sRNA Transcriptome in *Streptococcus pneumoniae* Serotype
576 2 Strain D39. *Journal of Bacteriology*, (2019).
577 14. J. Slager, R. Aprianto, J. W. Veening, Deep genome annotation of the opportunistic human
578 pathogen *Streptococcus pneumoniae* D39. *Nucleic Acids Research* **46**, 9971-9989
579 (2018).
580 15. H. C. Tsui *et al.*, Identification and characterization of noncoding small RNAs in
581 *Streptococcus pneumoniae* serotype 2 strain D39. *Journal of Bacteriology* **192**, 264-279
582 (2010).
583 16. A. Halfmann, M. Kovacs, R. Hakenbeck, R. Bruckner, Identification of the genes directly
584 controlled by the response regulator CiaR in *Streptococcus pneumoniae*: five out of 15
585 promoters drive expression of small non-coding RNAs. *Molecular Microbiology* **66**, 110-
586 126 (2007).
587 17. K. Hentrich *et al.*, *Streptococcus pneumoniae* Senses a Human-like Sialic Acid Profile via
588 the Response Regulator CiaR. *Cell Host Microbe* **20**, 307-317 (2016).
589 18. P. D. Rogers *et al.*, Gene expression profiling of the response of *Streptococcus pneumoniae*
590 to penicillin. *J Antimicrob Chemother* **59**, 616-626 (2007).
591 19. A. Schnorpfeil *et al.*, Target evaluation of the non-coding csRNAs reveals a link of the two-
592 component regulatory system CiaRH to competence control in *Streptococcus*
593 *pneumoniae* R6. *Molecular Microbiology* **89**, 334-349 (2013).
594 20. F. E. Jacobsen, K. M. Kazmierczak, J. P. Lisher, M. E. Winkler, D. P. Giedroc, Interplay
595 between manganese and zinc homeostasis in the human pathogen *Streptococcus*
596 *pneumoniae*. *Metallomics* **3**, 38-41 (2011).
597 21. J. E. Martin, J. P. Lisher, M. E. Winkler, D. P. Giedroc, Perturbation of manganese
598 metabolism disrupts cell division in *Streptococcus pneumoniae*. *Molecular Microbiology*
599 **104**, 334-348 (2017).
600 22. B. A. Eijkelkamp *et al.*, Extracellular zinc competitively inhibits manganese uptake and
601 compromises oxidative stress management in *Streptococcus pneumoniae*. *PloS one* **9**,
602 e89427 (2014).
603 23. A. L. McFarland, N. Bhattarai, M. Joseph, M. E. Winkler, J. E. Martin, Cellular Mn/Zn Ratio
604 Influences Phosphoglucomutase Activity and Capsule Production in *Streptococcus*
605 *pneumoniae* D39. *Journal of Bacteriology* **203**, e0060220 (2021).
606 24. C. A. McDevitt *et al.*, A molecular mechanism for bacterial susceptibility to zinc. *PLoS*
607 *Pathogens* **7**, e1002357 (2011).
608 25. J. E. Martin *et al.*, The zinc efflux activator SczA protects *Streptococcus pneumoniae*
609 serotype 2 D39 from intracellular zinc toxicity. *Molecular Microbiology* **104**, 636-651
610 (2017).
611 26. A. D. Ogunniyi *et al.*, Central role of manganese in regulation of stress responses,
612 physiology, and metabolism in *Streptococcus pneumoniae*. *Journal of Bacteriology* **192**,
613 4489-4497 (2010).

27. T. G. Kloosterman, M. M. van der Kooi-Pol, J. J. Bijlsma, O. P. Kuipers, The novel transcriptional regulator SczA mediates protection against Zn2+ stress by activation of the $Zn2^{+}$-resistance gene *czcD* in *Streptococcus pneumoniae*. *Molecular Microbiology* **65**, 1049-1063 (2007).
28. L. Bayle *et al.*, Zinc uptake by *Streptococcus pneumoniae* depends on both AdcA and AdcAII and is essential for normal bacterial morphology and virulence. *Molecular Microbiology* **82**, 904-916 (2011).
29. A. Dintilhac, G. Alloing, C. Granadel, J. P. Claverys, Competence and virulence of *Streptococcus pneumoniae*: Adc and PsaA mutants exhibit a requirement for Zn and Mn resulting from inactivation of putative ABC metal permeases. *Molecular Microbiology* **25**, 727-739 (1997).
30. C. D. Plumptre *et al.*, AdcA and AdcAII employ distinct zinc acquisition mechanisms and contribute additively to zinc homeostasis in *Streptococcus pneumoniae*. *Molecular Microbiology* **91**, 834-851 (2014).
31. J. W. Rosch, G. Gao, G. Ridout, Y. D. Wang, E. I. Tuomanen, Role of the manganese efflux system *mntE* for signalling and pathogenesis in *Streptococcus pneumoniae*. *Molecular Microbiology* **72**, 12-25 (2009).
32. J. E. Martin *et al.*, A Mn-sensing riboswitch activates expression of a Mn^{2+}/Ca^{2+} ATPase transporter in Streptococcus. *Nucleic Acids Research* **47**, 6885-6899 (2019).
33. R. Novak, J. S. Braun, E. Charpentier, E. Tuomanen, Penicillin tolerance genes of *Streptococcus pneumoniae*: the ABC-type manganese permease complex Psa. *Molecular Microbiology* **29**, 1285-1296 (1998).
34. N. S. Jakubovics, A. W. Smith, H. F. Jenkinson, Expression of the virulence-related Sca (Mn^{2+}) permease in *Streptococcus gordonii* is regulated by a diphtheria toxin metallorepressor-like protein ScaR. *Molecular Microbiology* **38**, 140-153 (2000).
35. J. W. Johnston, D. E. Briles, L. E. Myers, S. K. Hollingshead, Mn^{2+}-dependent regulation of multiple genes in *Streptococcus pneumoniae* through PsaR and the resultant impact on virulence. *Infection and Immunity* **74**, 1171-1180 (2006).
36. S. Lacks, R. D. Hotchkiss, A study of the genetic material determining an enzyme in Pneumococcus. *Biochim Biophys Acta* **39**, 508-518 (1960).
37. S. Ramos-Montanez *et al.*, Polymorphism and regulation of the *spxB* (pyruvate oxidase) virulence factor gene by a CBS-HotDog domain protein (SpxR) in serotype 2 *Streptococcus pneumoniae*. *Molecular Microbiology* **67**, 729-746 (2008).
38. K. E. Bruce, B. E. Rued, H. T. Tsui, M. E. Winkler, The Opp (AmiACDEF) Oligopeptide Transporter Mediates Resistance of Serotype 2 *Streptococcus pneumoniae* D39 to Killing by Chemokine CXCL10 and Other Antimicrobial Peptides. *Journal of Bacteriology* **200**, (2018).
39. K. M. Kazmierczak, K. J. Wayne, A. Rechtsteiner, M. E. Winkler, Roles of rel_{Spn} in stringent response, global regulation and virulence of serotype 2 *Streptococcus pneumoniae* D39. *Molecular Microbiology* **72**, 590-611 (2009).
40. B. Langmead, S. L. Salzberg, Fast gapped-read alignment with Bowtie 2. *Nature Methods* **9**, 357-359 (2012).
41. S. Anders, P. T. Pyl, W. Huber, HTSeq--a Python framework to work with high-throughput sequencing data. *Bioinformatics* **31**, 166-169 (2015).
42. M. I. Love, W. Huber, S. Anders, Moderated estimation of fold change and dispersion for RNA-seq data with DESeq2. *Genome Biol* **15**, 550 (2014).
43. D. Sinha, J. P. Frick, K. Clemons, M. E. Winkler, N. R. De Lay, Pivotal Roles for Ribonucleases in *Streptococcus pneumoniae* Pathogenesis. *mBio*, e0238521 (2021).
44. Y. Fu *et al.*, A new structural paradigm in copper resistance in *Streptococcus pneumoniae*. *Nat Chem Biol* **9**, 177-183 (2013).

666 **FIGURES**

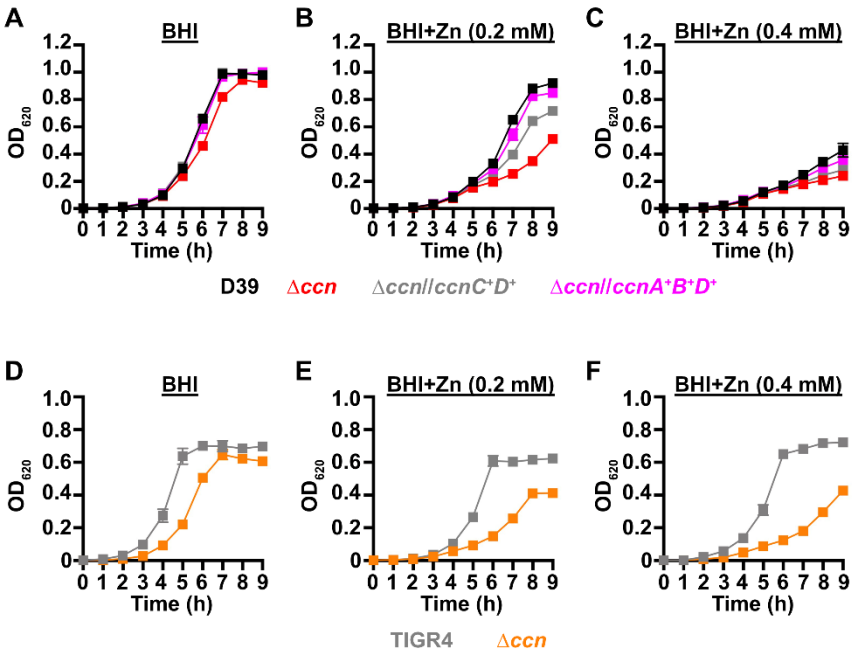

667

668 **Figure 1:** Growth phenotypes of *S. pneumoniae* strains harboring deletion of the *ccn* genes.
669 Growth characteristics at 37°C under an atmosphere of 5% CO_2 in BHI broth alone (A, D) or with
670 0.2 mM (B, E) or 0.4 mM (C,F) $ZnSO_4$ of following strains: (A, B, C) IU781 (D39), NRD10176
671 (Δ*ccn*), NRD10396 (Δ*ccn//ccnA*$^+$*B*$^+$*D*$^+$), and NRD10397 (Δ*ccn//ccnC*$^+$*D*$^+$); (D, E, F) NRD10220
672 (TIGR4) and NRD10266 (Δ*ccn*). Each point on the graph represents the mean OD_{620} value from
673 three independent cultures. Error bars, which in some cases are too small to observe in the graph,
674 represent the standard deviation (SD).

675

676

677

678

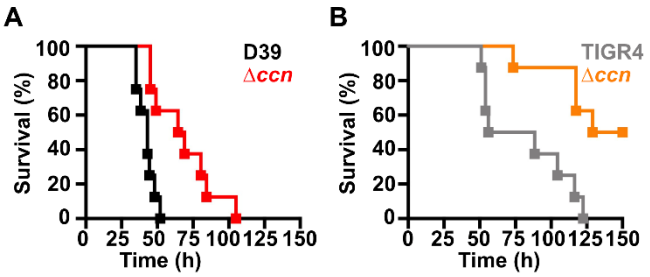

Figure 2: Virulence phenotypes of *S. pneumoniae* strains harboring deletion of the *ccn* genes. Survival curve of ICR outbred mice after infection with ~10^7 CFU in a 50 μL inoculum of the following *S. pneumoniae* strains: (A) IU1781 (D39 *rpsL1*) and NRD10176 (Δ*ccn rpsL1*); (C) NRD10220 (TIGR4 *rpsL1*) and NRD10266 (Δ*ccn rpsL1*). The difference in median survival time of IU1781 vs NRD10176 (43.0 h vs 66.8 h) and NRD10220 vs NRD10266 (72.3 h vs 139.5 h) were statistically significant, P = 0.0015 and P = 0.0018, respectively. Eight mice were infected per strain. Disease progression of animals was monitored, the time at which animals reached a moribund state was recorded, and these mice were subsequently euthanized as described in Materials and Methods. A survival curve was generated from this data and analyzed by Kaplan-Meier statistics and log rank test to determine P-values.

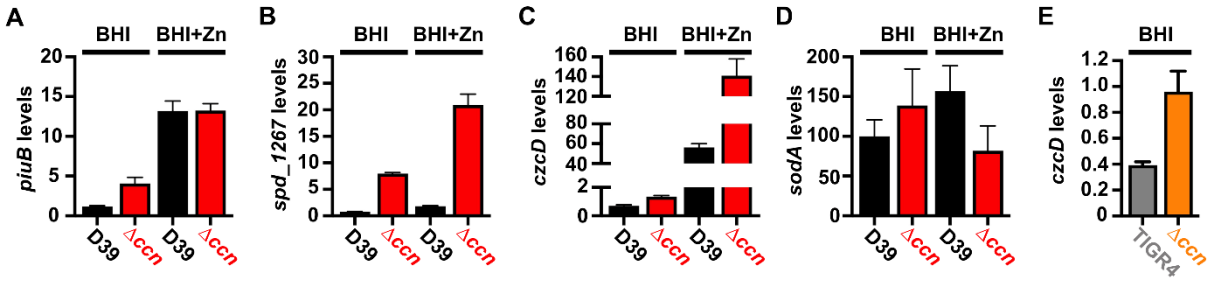

Figure 3: Loss of the *ccn* genes perturbs the expression of Zn and Mn stress associated genes in *S. pneumoniae*. Abundance of *piuB* (A), *spd_1267* (B), *czcD* (C, E), and *sodA* (D) mRNAs was determined by RT-ddPCR (A, B, and C) or northern blot analyses (D) as described in Materials

696 and Methods for strain IU1781 (D39) and derived Δ*ccnABCDE* mutant strain (NRD10176; Δ*ccn*)
697 grown to exponential phase (OD_{620} of ~0.2) in BHI broth alone (BHI) or supplemented with 0.2
698 mM $ZnSO_4$ (BHI+Zn) at 37°C under an atmosphere of 5% CO_2. (E) Expression of *czcD* was
699 determined by RT-ddPCR analyses for NRD10220 (TIGR4) and derived Δ*ccnABCDE* mutant
700 strain NRD10266 (Δ*ccn*) grown to exponential phase in BHI Broth at 37°C under an atmosphere
701 of 5% CO_2. Transcript levels were normalized to *tuf* (A, B, C, and E) or 5S rRNA (D). Values
702 represent the mean of three independent cultures and error bars indicate SEM.

703

704

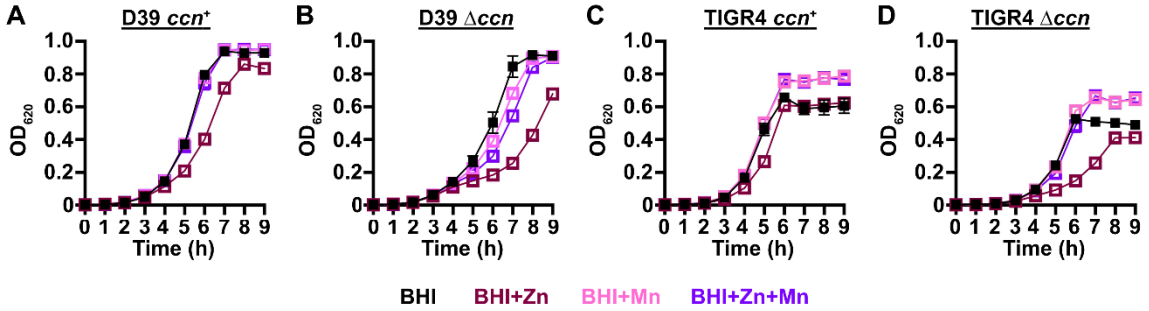

705

706 **Figure 4:** Mn supplementation eliminates the Zn dependent growth inhibition of *S. pneumoniae*
707 Δ*ccnABCDE* mutant. Growth characteristics at 37°C under an atmosphere of 5% CO_2 in BHI broth
708 alone (BHI) or with 0.2 mM $ZnSO_4$ (BHI+Zn), 0.2 mM $MnCl_2$ (BHI+Mn), or 0.2 mM $ZnSO_4$ and
709 $MnCl_2$ (BHI+Zn+Mn) of strains (A) IU1781 (D39 *ccn*$^+$), (B) NRD10176 (D39 Δ*ccn*), (C), NRD10220
710 (TIGR4 *ccn*$^+$), and (D) NRD10266 (TIGR4 Δ*ccn*). Each point on the graph represents the mean
711 OD_{620} value from three independent cultures. Error bars, which in some cases are too small to
712 observe in the graph, represent the standard deviation (SD).

713

714

715

716

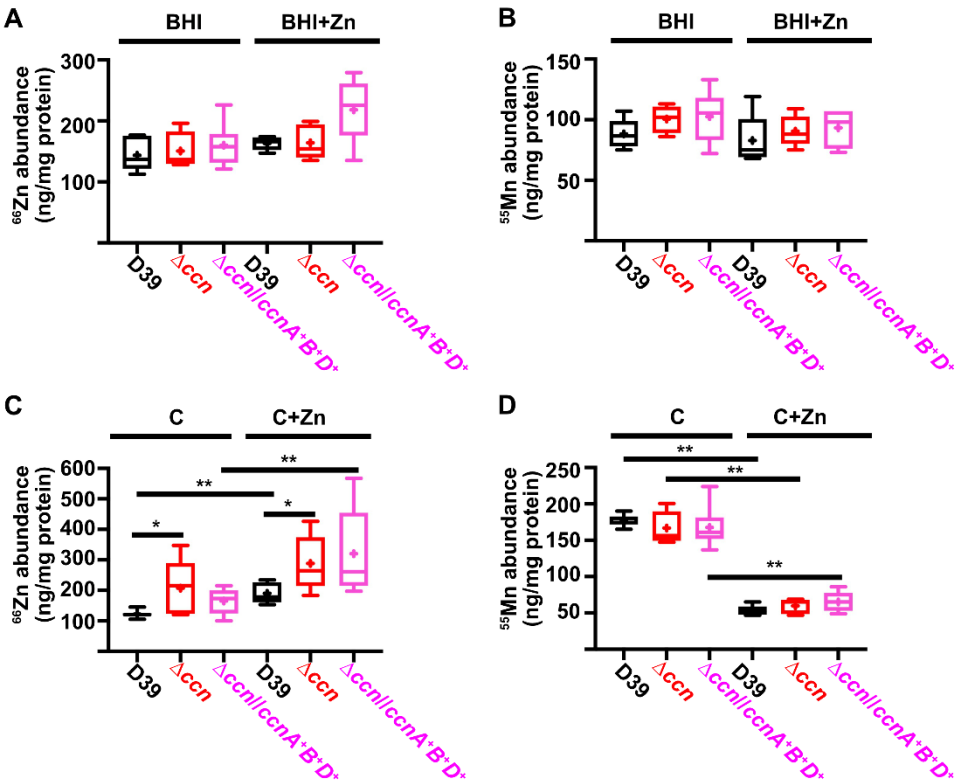

Figure 5: Deletion of the *ccn* genes increases total cell-associated Zn levels, but not Mn levels, in C medium. Total cell associated Zn (A, C) and Mn (B, D) abundance was measured from cells harvested from cultures of IU781 (D39), NRD10176 (Δ*ccn*), and NRD10396 (Δ*ccn*//*ccnA*$^+$*B*$^+$*D*$^+$) grown to exponential growth phase (OD_{620} of ~0.2) in BHI broth (BHI) or BHI broth with 0.2 mM $ZnSO_4$ (BHI+Zn) (A and B) or in C medium (C) or C medium with 0.2 mM $ZnSO_4$ (C+Zn) (C and D) by ICP-MS and normalized to protein amounts. Results presented in box and whisker plots represent the median of 5 to 8 replicates with whiskers indicating the 5-95% percentile. Means are indicated by "+". Statistical analysis was performed using a Mann-Whitney test, and statistically significant results are indicated by * ($P < 0.05$) or ** ($P < 0.05$).

731

732

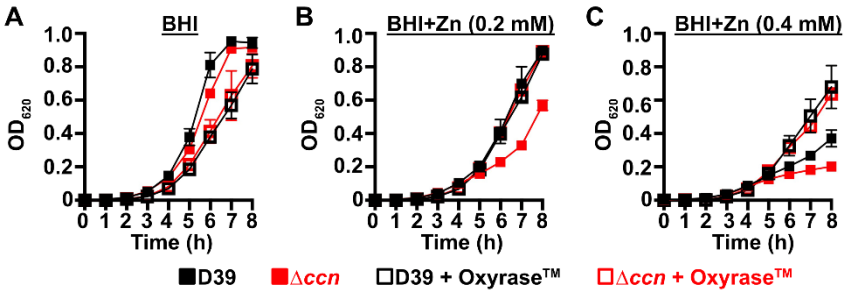

733

734 **Figure 6:** Reduction of O_2 abolishes the Zn hypersensitivity of the *S. pneumoniae* Δ*ccnABCDE*

735 mutant. Growth characteristics at 37°C under an atmosphere of 5% CO_2 in BHI broth alone (A)

736 or with 0.2 mM (B) or 0.4 mM (C) $ZnSO_4$ of IU781 (D39) and NRD10176 (Δ*ccn*) in the absence

737 or presence of 10% (volume/volume) Oxyrase™. Each point on the graph represents the mean

738 OD_{620} value from three independent cultures. Error bars, which in some cases are too small to

739 observe in the graph, represent the standard deviation (SD).

740

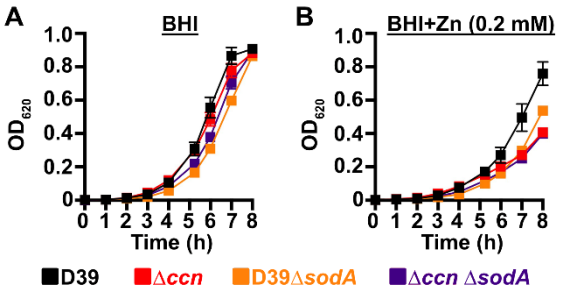

741

742

743 **Figure 7: A *S. pneumoniae* Δ*sodA* mutant phenocopies the Zn hypersensitivity of a**

744 **Δ*ccnABCDE* mutant strain.** Growth characteristics at 37°C under an atmosphere of 5% CO_2 in

745 BHI broth alone (A) or with 0.2 mM $ZnSO_4$ (B) of IU781 (D39), NRD10176 (Δ*ccn*), NRD10533

746 (D39 Δ*sodA*), and NRD10534 (Δ*ccn* Δ*sodA*). Each point on the graph represents the mean

747 OD_{620} value from three independent cultures. Error bars, which in some cases are too small to

748 observe in the graph, represent the standard deviation (SD).